American Journal of Pathology, Vol. 155, No. 6, December 1999

Blood-Brain Barrier Tight Junction Disruption in Human Immunodeficiency Virus-1 Encephalitis

Linda M. Dallasta,* Liubomir A. Pisarov,* James E. Esplen,* Jonette V. Werley,* Ashlee V. Moses,† Jay A. Nelson,† and Cristian L. Achim*

From the Department of Pathology, Division of Neuropathology, University of Pittsburgh School of Medicine, Pittsburgh, Pennsylvania; and the Department of Microbiology and Immunology,† Oregon Health Sciences University, Portland, Oregon*

The blood-brain barrier (BBB) plays a critical role in regulating cell trafficking through the central nervous system (CNS) due to several unique anatomical features, including the presence of interendothelial tight junctions that form impermeable seals between the cells. Previous studies have demonstrated BBB perturbations during human immunodeficiency virus encephalitis (HIVE); however, the basis of these permeability changes and its relationship to infiltration of human immunodeficiency virus type 1 (HIV-1)-infected monocytes, a critical event in the pathogenesis of the disease, remains unclear. In this study, we examined CNS tissue from HIV-1-seronegative patients and HIV-1-infected patients, both with and without encephalitis, for alterations in BBB integrity via immunohistochemical analysis of the tight junction membrane proteins, occludin and zonula occludens-1 (ZO-1). Significant tight junction disruption ($P < 0.001$), as demonstrated by fragmentation or absence of immunoreactivity for occludin and ZO-1, was observed within vessels from subcortical white matter, basal ganglia, and, to a lesser extent, cortical gray matter in patients who died with HIVE. These alterations were also associated with accumulation of activated, HIV-1-infected brain macrophages, fibrinogen leakage, and marked astrocytosis. In contrast, no significant changes ($P > 0.05$) were observed in cerebellar tissue from patients with HIVE compared to HIV-seronegative patients or HIV-1-infected patients without encephalitis. Our findings demonstrate that tight junction disruption is a key feature of HIVE that occurs in regions of histopathological alterations in association with perivascular accumulation of activated HIV-1-infected macrophages, serum protein extravasation, and marked astrocytosis. We propose that disruption of this key BBB structure serves as the main route of HIV-1-infected monocyte entry into the CNS. ***(Am J Pathol 1999, 155:1915–1927)***

Human immunodeficiency virus type 1 (HIV-1)-associated dementia complex[1] is a syndrome of progressive motor, cognitive, and behavioral impairment that occurs in a significant number of patients with acquired immunodeficiency syndrome (AIDS) late in the course of their infection.[2,3] The neuropathological correlate, HIV-1 encephalitis (HIVE),[4] is characterized by subcortical and neocortical damage within the white and gray matter.[5,6] Pathological hallmarks include the formation of multinucleated giant cells and microglial nodules, as well as a striking perivascular and parenchymal accumulation of macrophages.[7] In addition, widespread reactive astrocytosis, diffuse white matter pallor, and varying degrees of neuronal injury and loss are present. These changes are associated with both increasing CNS viral burden,[8] as well as the presence of activated, HIV-1-infected infiltrating macrophages and resident microglia, the primary central nervous system (CNS) targets of HIV-1.[9–12] Although viral expansion is requisite for the development of HIVE, recent studies indicate that the number of activated macrophages and microglia may also serve as a good indicator for the level of neurological dysfunction.[13] Indeed, the vast array of secretory products released by these activated cells is now considered to be the basis of HIV-1-associated neurotoxicity.[14–19]

The entry of HIV-1-infected monocytes into the CNS is hypothesized to occur through breaches in the blood-brain barrier (BBB). The BBB is composed of a network of continuous capillaries surrounded by a basal lamina and astrocytic foot processes.[20] Under physiological conditions, this vascular barrier selectively regulates the intracellular and paracellular exchange of macromolecules and cells between the circulation and CNS through several unique structural and functional attributes. These include specialized endothelial membrane transport systems,[21] limited endothelial pinocytosis, and lack of transendothelial fenestrae.[22] Most distinct is the presence of high resistance interendothelial zonula occludens, or tight junctions.[23,24] These intercellular belts consist of continuous, anastomosing intramembranous strands[25] between the outer leaflets of adjacent cerebral endothelial cell membranes and are composed, in part, of a number of proteins, including the integral membrane pro-

Supported by National Institutes of Health grant NS 35419 to C. L. A.

Accepted for publication August 24, 1999.

Address reprint requests to Linda M. Dallasta, M.D., Ph.D., Division of Neuropathology, Presbyterian University Hospital, A-515, 200 Lothrop Street, Pittsburgh, PA 15213-2582. E-mail: dallasta@np.awing.upmc.edu.

tein, occludin[26,27] and the peripheral membrane protein, zonula occludens-1 (ZO-1).[28] Unlike systemic endothelial and epithelial tight junctions, cerebral endothelial tight junctions lack pore-like discontinuities,[29] and, hence, create impermeable seals between the cells. In total, these barrier features serve to restrict the exchange between the microvasculature and CNS and, in particular, regulate inflammatory cell egress from the circulation.

During HIV-1 infection, however, multiple studies demonstrate that this strictly regulated exchange is compromised. In clinical studies of HIV-1-infected patients, tomographic analyses show perfusion defects[30–32] compatible with cerebral vascular compromise, whereas both computed tomography and magnetic resonance imaging (MRI) studies reveal abnormal white matter signals[33–35] that do not correspond to regions of demyelination.[36] Elevated cerebrospinal fluid (CSF) markers of BBB damage, including increased CSF-serum albumin ratios,[37,38] matrix metalloproteinase levels,[39] and nitric oxide metabolites,[40] also occur in HIV-1-infected patients. Serum protein extravasation through the BBB occurs in the brains of patients with HIV and HIVE,[36,41,42] accompanied by abnormal neuronal and glial immunoreactivity for these proteins. In addition, morphological changes develop in the cerebral endothelium, including endothelial hypertrophy,[43] membrane glycoprotein loss,[44] and basal lamina thinning.[45] Furthermore, functional alterations occur in the levels of the membrane glucose transporter-1,[46] a barrier-related protein.

Although these observations clearly demonstrate that both structural and functional BBB perturbations occur during HIV-1 infection, the precise mechanism of these permeability changes and their relationship to the entry of HIV-1-infected monocytes into the CNS remain unclear. To gain insight into this issue, we examined tight junction integrity in autopsy CNS tissue from HIV-1-infected patients, both with and without encephalitis, as well as tissue from HIV-1-seronegative patients. Tight junctions were assessed immunohistochemically for changes in occludin and ZO-1 expression within the frontal cortex and basal ganglia, regions demonstrating histopathological features of HIVE and high HIV-1 burden and associated pathology.[47] This expression was compared to that in the cerebellum, a region demonstrating no or minimal HIV-1 burden.[47] These changes, in turn, were correlated with BBB permeability, astrocytosis, monocyte accumulation, and viral burden via assessment of fibrinogen, glial fibrillary acid protein (GFAP), CD68, and HIV-1 gp41 immunoreactivity. Our findings demonstrate that significant tight junction disruption, as demonstrated by fragmentation or absence of immunoreactivity for the proteins occludin and ZO-1, is a fundamental feature of HIVE. We further demonstrate that these BBB changes occur in regions of histopathological damage in concert with perivascular accumulation of activated, HIV-1-infected monocytes and microglia, serum protein extravasation, and abundant astrogliosis. We propose that disruption of this critical barrier structure serves as the primary portal of entry whereby activated HIV-1-infected monocytes gain access to the CNS.

Materials and Methods

Tissues

Six brains from patients with AIDS (mean age 34 ± 6 years; mean HIV-1 seropositivity 6 ± 3 years) and ten brains from patients with HIVE (mean age 40 ± 7 years; mean HIV-1 seropositivity 5 ± 4 years) were selected from our previous study set of 74 consecutive brain-inclusive AIDS autopsies between March, 1981 and July, 1996 at the Presbyterian University Hospital, University of Pittsburgh Medical Center.[48] Clinical and pathological data were obtained from the patients' medical records and autopsy reports, including the date of the first AIDS-defining illness (according to the 1987 Centers for Disease Control criteria). AIDS-dementia complex was defined by HIV-1 seropositivity accompanied by a clinical history and neurological findings of progressive cognitive and/or motor impairment in the absence of opportunistic infection. All selected patients with AIDS and AIDS-dementia complex were male. Risk factors included homosexuality (12), bisexuality (2), intravenous drug abuse (1), and blood transfusions (1). Causes of death in the AIDS group included pneumonia (5) and complications of disseminated Kaposi's sarcoma (1). Causes of death in the AIDS-dementia complex group included pneumonia (7), multi-organ failure (2), and acute hemorrhage (1).

Nine brains from HIV-1-seronegative patients (mean age 52 ± 15 years) were selected as controls. Causes of death included cardiac arrhythmias or heart failure (3), diffuse alveolar damage (1), alcohol-induced cirrhosis (1), cerebral and pulmonary fat emboli (1), acute supporative meningitis (1), Pick's disease (1), and complications of chronic multiple sclerosis (1).

Light Microscopy

Autopsies from patients with AIDS and AIDS-dementia complex were performed with a mean postmortem interval of 8.8 ± 6.2 hours and 12.3 ± 6.4 hours, respectively. Autopsies from control patients were performed with a mean postmortem interval of 13.4 ± 8.2 hours. Brains were fixed in 10% formalin for 10 to 14 days before sectioning. Samples from the following regions were paraffin-embedded and stained with hematoxylin and eosin for routine histopathological examination: mid-frontal cortex, caudate nucleus, insular cortex, basal ganglia, thalamus, hippocampus, cerebellum, midbrain, pons, medulla, and spinal cord. Microscopic examination and immunohistochemical stains revealed no evidence of opportunistic infection or neoplasms, including lymphoma. Sections from the mid-frontal cortex, basal ganglia, and cerebellum were then selected for this study.

Tissue sections from the cortical gray matter, subcortical and deep white matter, and deep gray matter were examined for the distribution and abundance of HIV-1 proteins by immunohistochemical staining for gp41, the transmembrane portion of the HIV-1 envelope protein, as previously described.[48] In brief, levels of gp41 expression were assessed separately for each region (an average of five fields per region per 20× microscopic objec-

Table 1. Panel of Antibodies Used for Immunohistochemistry

Antibody	Specificity	Manufacturer	Host/class	Dilution
Occludin	Integral membrane protein of epithelial and endothelial tight junctions (26)*	Zymed, San Francisco, CA	Rabbit Ig	1:250
ZO-1	Peripheral membrane protein of epithelial and endothelial tight junctions (28, 49)* and adherens junctions (50)*	Zymed	Rabbit Ig	1:250
Fibrinogen	Plasma protein	Dako, Carpinteria, CA	Rabbit Ig	1:10,000
Human Glial Fibrillary Acidic Protein (GFAP)	Astrocytes, some ependymal cells	Dako (Clone 6F2)	Mouse IgG_1	1:50
CD68	Peripheral blood mononuclear cells and tissue macrophages, including microglia	Dako (Clone PG-M1)	Mouse IgG_3	1:100
Human CD34	Endothelial cells, hematopoietic cells, collagen IV	Biogenex, San Ramon, CA (Clone QBEnd/10)	Mouse IgG_1	Neat
HLA-DR	Major histocompatibility Class II antigens	Pharmingen, San Diego, CA (Clone 4U39)	Mouse IgG_{2a}	1:50
gp41	Transmembrane portion of HIV-1 envelope protein	Genetic Systems, Seattle, WA	Mouse IgG_1	1:750

*Numbers in parentheses correspond to references.

tive) and scored on a scale of 0 to 2 as follows: 0 = no cells stained for gp41, 1 = less than 2 cells stained for gp41, 2 = more than 2 cells stained for gp41. A composite score, derived by adding individual scores of the three regions, was scored on a scale of 0 to 6 as follows: 0–1 = absent to minimal HIV-1 burden, 2–3 = moderate HIV-1 burden, 4–6 = abundant HIV-1 burden. In sections from all patients with AIDS-dementia complex, gp41-immunoreactive cells with microglial or macrophage morphology were most prevalent in the deep gray matter (average gp41 score 2.0 ± 0.0), followed by the cortical white matter (average gp41 score 1.7 ± 0.7) and cortical gray matter (average gp41 score 0.9 ± 0.9). The gp41 composite score for all cases was 4.6 ± 1.2, with 90% of the cases demonstrating an abundant HIV-1 burden and 10% a moderate HIV-1 burden.

Immunoperoxidase Staining

Paraffin-embedded tissue sections were deparaffinized in Histoclear (National Diagnostics, Atlanta, GA), rehydrated, and treated with 3% hydrogen peroxide (Sigma Chemical Co., St. Louis, MO) for 30 minutes. Sections requiring antigen retrieval were treated with either pepsin (0.4%; Dako Corporation, Carpinteria, CA) at 37°C for 10 minutes or Citra solution (Biogenex, San Ramon, CA) for 3 to 7 minutes using the recommended microwave protocol. Sections were rinsed with phosphate-buffered saline (PBS) and incubated in TNB blocking buffer (DuPont NEN, Boston, MA) for 30 minutes. After overnight incubation at 4°C with primary antibody (Table 1), the sections were rinsed in PBS and then incubated at room temperature for 1 hour with either biotinylated goat anti-mouse immunoglobulin G (IgG) serum (1:100; Caltag Laboratories, Burlingame, CA) or goat anti-rabbit Ig (1:200; Biogenex). Immunostaining was then performed using the tyramide signal amplification method according to the manufacturer's protocol (biotinylated tyramide, 1:150, 10 minutes; TSA-Indirect, DuPont NEN). Chromagen reactions were developed with 3-amino-9-ethylcarbazole (AEC; Biogenex) and counterstained with Mayer's hematoxylin. Isotype-matched normal mouse serum was used as a negative reagent control.

Sections were analyzed semiquantitatively with an Olympus BX40F-3 microscope (Tokyo, Japan) and photographed with an Olympus SC35 camera. Vessels demonstrating strong, continuous interendothelial reactivity for either occludin or ZO-1 were considered positive, and vessels demonstrating weak, fragmented, or no expression of either occludin or ZO-1 were considered negative. An average of five fields of blood vessels was counted separately for each region with a micrometer and a 20× microscopic objective. Sections from a patient with chronic multiple sclerosis showed no tight junction protein expression on blood vessels within burned-out plaques, and, thus, served as a negative control. Strong expression of both markers was present on vessels in the surrounding, uninvolved parenchyma, however, and these areas were used for quantification. Blood vessels showing CD34 reactivity or intravascular fibrinogen reactivity without extravasation were counted in a similar manner. Statistical analysis was performed using the unpaired Student's *t*-test, where two-tailed P values <0.05 were considered significant, P values <0.01 were considered very significant, and P values <0.0001 were considered highly significant.

Double Immunofluorescence Staining

Paraffin-embedded sections were treated with the same protocol as described for immunoperoxidase staining. Following overnight incubation at 4°C with the primary antibody (Table 1), the sections were rinsed with PBS and incubated at room temperature for 1 hour with either

biotinylated goat anti-mouse immunoglobulin G (IgG) serum (1:100; Caltag Laboratories) or goat anti-rabbit Ig (1:200; Biogenex). Immunofluorescent staining was performed using the tyramide signal amplification method according to the manufacturer's protocol tetramethylrhodamine isothiocyanate (TRITC)-labeled tyramide, 1:100, 10 minutes; excitation peak 570 nm; emission peak 590 nm; TSA-Direct, DuPont NEN). Sections were then incubated with the second primary antibody at room temperature for 2 hours. After rinsing in PBS, sections were incubated at room temperature for 1 hour with either fluorescein isothiocyanate (FITC)-labeled donkey anti-rabbit Ig (1:100; Jackson ImmunoResearch Laboratories, West Grove, PA) or FITC-labeled goat anti-mouse IgG (1:100; Jackson). Immunostaining was then performed using the tyramide signal amplification method according to the manufacturer's protocol (FITC-labeled tyramide, 1:100, 10 minutes; TSA-Indirect, DuPont NEN). Isotype-matched normal mouse serum was used as a negative reagent control.

Confocal Microscopy

Double-labeled immunofluorescent sections were analyzed with a Molecular Dynamics laser scanning confocal microscope (Sunnyvale, CA) equipped with an argon/krypton laser, Nikon inverted microscope, and Plan Apo 20× 0.75 NA (air) and Plan Apo 60× 1.40 NA (oil) objective lenses. FITC and TRITC were excited by the laser's 488-nm and 568-nm lines, respectively, which were delivered to the tissue sections by a 488/568 B/S primary dichroic beamsplitter. Fluorescent light emitted by FITC and TRITC was separated by a 565 B/S secondary dichroic beamsplitter and then passed through a 530DF30 filter and a 600DF40 filter, respectively. Images were collected with a Silicon Graphics Inc. computer (Operating System release 5.3, Farmington, MI) and analyzed using the Image Space software (version 3.2, Molecular Dynamics).

Results

The Distribution of Tight Junction Proteins Is Disrupted in HIVE

Blood vessels were examined immunohistochemically for changes in tight junction protein expression and distribution using antibodies to the tight junction markers, occludin, an integral membrane protein, and ZO-1, a peripheral membrane protein. In addition, vascular density was assessed by immunostaining for CD34, an endothelial cell marker.

All size blood vessels from all regions in control sections demonstrated a strong, continuous interendothelial staining pattern (Figure 1A) of equal intensity when stained for either tight junction protein (occludin immunostaining is shown in Figure 1; similar reactivity patterns were seen with ZO-1 immunostaining, data not shown). Although regional variations in vascular density were observed (Figure 2A), no statistically significant differences ($P > 0.05$) were noted in the mean number of occludin- or ZO-1-reactive blood vessels (Figure 2, B and C) compared to the mean number of CD34-reactive blood vessels within the same region (Figure 2A).

Sections from HIV-1 patients without HIVE showed no differences in vascular density when compared to the same regions in control sections (Figure 2A). Similarly, sections from HIV-1 patients without HIVE demonstrated strong, continuous interendothelial expression of both occludin and ZO-1 on all cerebellar blood vessels, as well as a majority of vessels in the cortical gray matter, cortical white matter, and deep gray matter. Scattered, isolated medium-sized blood vessels in the cortical white matter, the globus pallidus and, less frequently, the cortical gray matter, however, showed weak or fragmented expression of these markers (Figure 1B). Single, weakly cross-reactive cells with astrocytic morphology (Figure 1B) surrounded occasional altered vessels in regions of mild, diffuse gliosis. Overall, however, no statistically significant difference ($P > 0.05$) was observed in the mean number of occludin or ZO-1-reactive blood vessels in these regions compared to the same regions in control sections (Figure 2, B and C).

In contrast, despite comparable regional vascular densities (Figure 2A), sections from patients with HIVE showed marked alterations in both the intensity and staining pattern of occludin and ZO-1 when compared to either control or HIV-1 sections. A majority of small and medium-sized vessels in the cortical white matter and deep gray matter showed either weak, fragmented expression or no expression of these markers (Figure 1, C and E). Isolated, similar-sized vessels with strong, continuous occludin or ZO-1 reactivity were often observed in the vicinity (Figure 1E). Nonetheless, highly statistically significant differences ($P < 0.0001$) were observed in the mean number of occludin- or ZO-1-reactive blood vessels in these regions compared to the same regions in either control or HIV-1 sections (Figure 2, B and C).

Numerous small and medium-sized vessels in the cortical gray matter from patients with HIVE showed similar alterations in the intensity and staining pattern of occludin or ZO-1, although to a lesser degree than that observed in the cortical white matter and deep gray matter (Figure 1D). Compared to the mean number of occludin- or ZO-1-reactive blood vessels in the cortical gray matter in either control or HIV-1 sections, however, very significant decreases ($P < 0.001$) in expression of these markers were observed (Figure 2, B and C). On the other hand, only focal vascular alterations in occludin or ZO-1 expression were observed in the cerebellar cortex or cerebellar white matter in patients with HIVE. Likewise, no statistically significant difference ($P > 0.05$) was observed in the mean number of occludin or ZO-1-reactive blood vessels in these regions compared to the same regions in either control or HIV-1 sections (Figure 2, B and C).

Histopathological features of HIVE were most pronounced in the deep gray matter and cortical white matter, followed by the cortical gray matter, and were, likewise, spatially associated with alterations in the vascular expression of both occludin and ZO-1 (Figure 1, D–F). Mononuclear cell aggregates and multinucleated giant

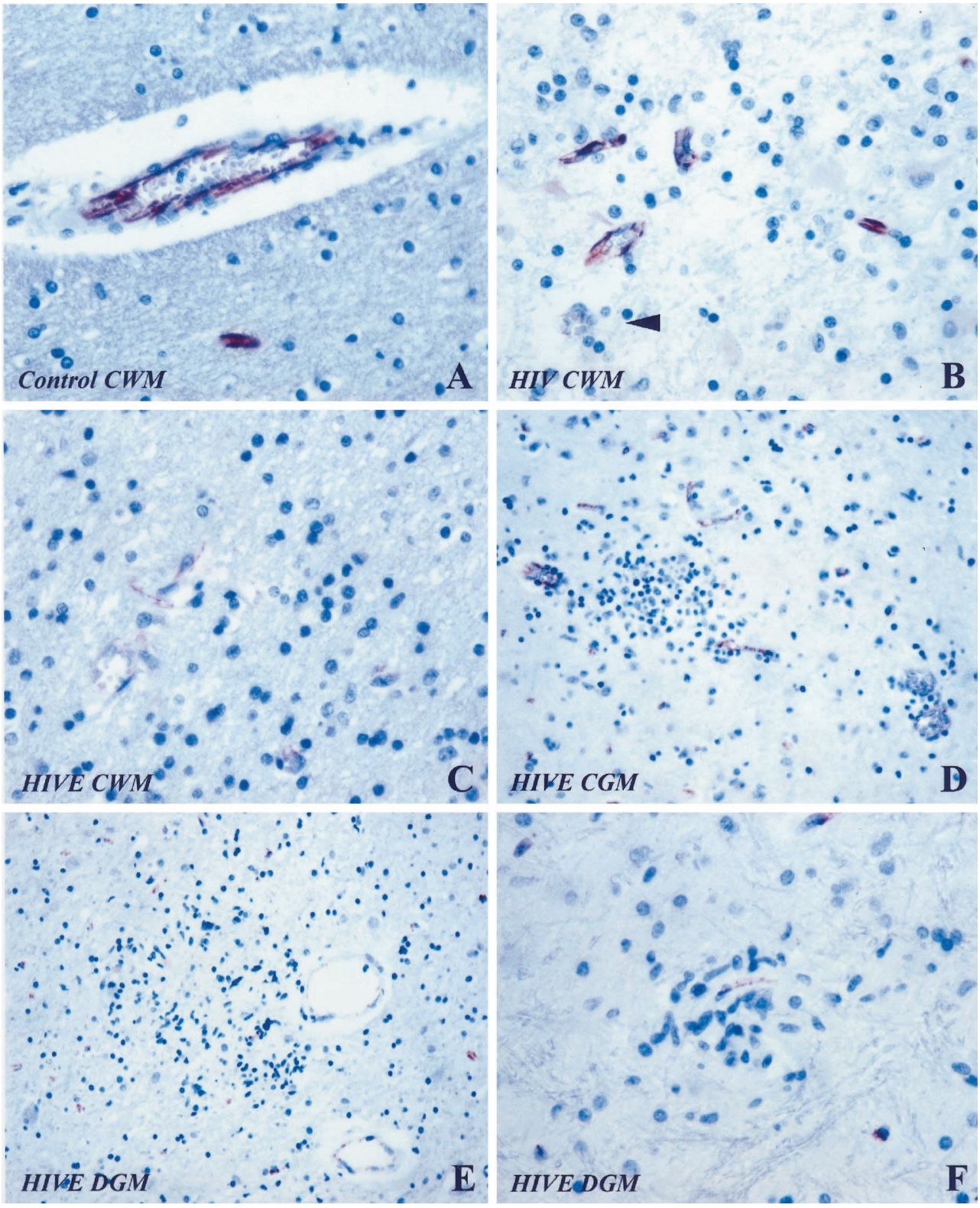

Figure 1. The distribution of tight junction proteins is disrupted in HIVE. **A:** In control sections, blood vessels show strong immunoreactivity for the tight junction-associated protein, occludin, in a continuous, interendothelial staining pattern. **B:** In HIV sections, isolated medium-sized vessels are weakly immunoreactive for occludin (**arrowhead**). **C–F:** In HIVE sections, numerous small and medium-sized vessels exhibit decreased to absent occludin immunoreactivity (**C**) in association with microglial nodules (**D** and **F**), mononuclear cell infiltrates (**D** and **E**), and multinucleated giant cells (**E**). Similar changes were observed in ZO-1-immunostained sections. **D** and **E:** Original magnification, ×200. **A–C** and **F:** Original magnification, ×400. CGM, cortical gray matter; CWM, cortical white matter; DGM, deep gray matter.

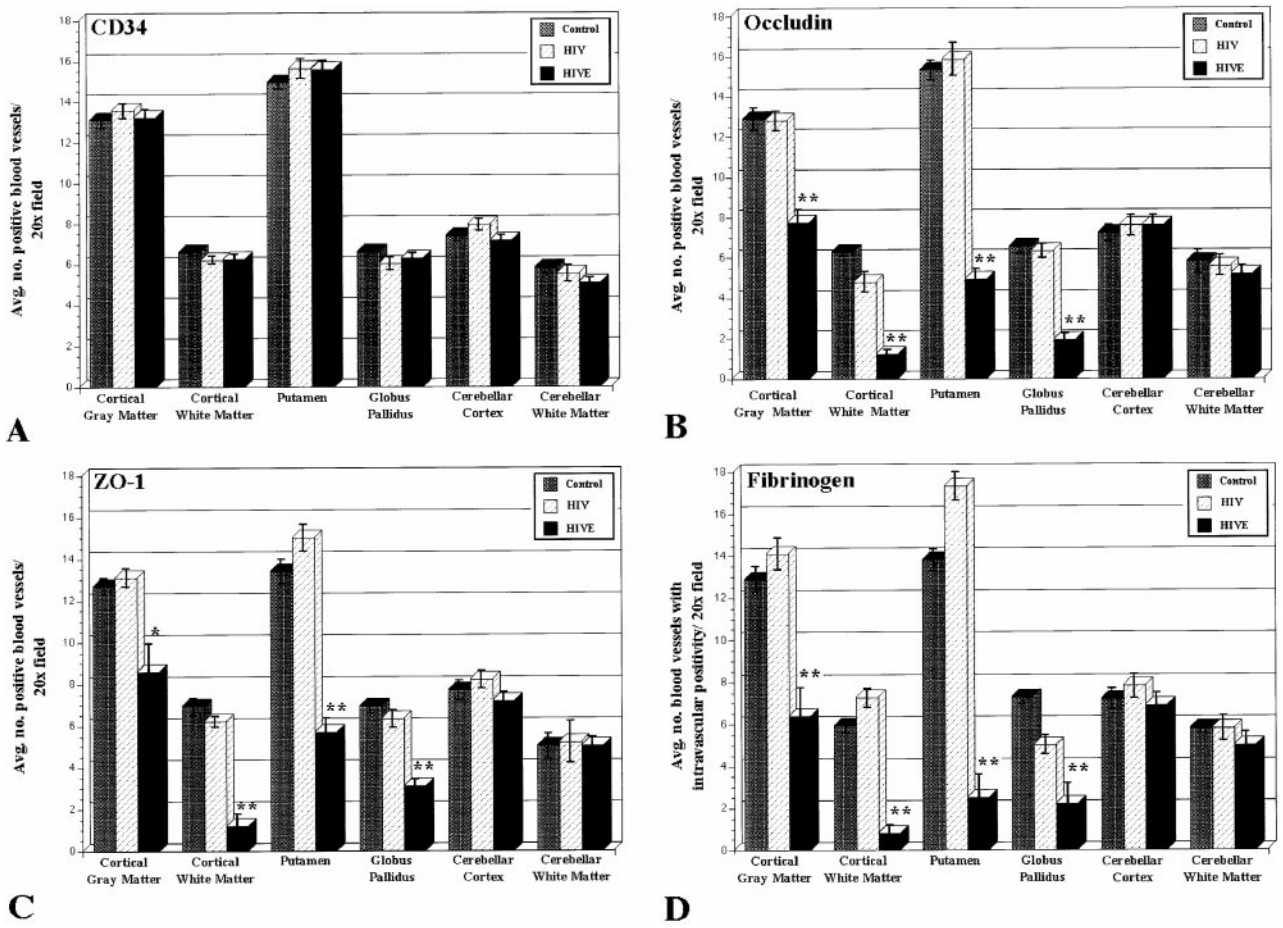

Figure 2. Semiquantitative analysis of blood vessel immunoreactivity for the endothelial cell marker, CD34 (**A**), the tight junction proteins, occludin (**B**) and ZO-1 (**C**), and the intravascular serum protein, fibrinogen (**D**), in sections from control, HIV, and HIVE brains (average and standard error of five fields of blood vessels per 20× objective). Two-tailed *P* values of <0.01 (*) and <0.0001 (**) are noted.

cells were frequently associated with vessels demonstrating alterations in tight junction protein expression (Figure 1E). Microglial nodules (Figure 1D), present in 20% of the cases, were also seen adjacent to vessels with weak, fragmented, or absent expression of either occludin or ZO-1. In addition, microglial nodules occasionally engulfed blood vessels with occludin- or ZO-1-positive vascular remnants (Figure 1F).

Tight Junction Protein Disruption Is Associated with Serum Protein Extravasation and Astrocytosis in HIVE

Sections were examined immunohistochemically for structural and functional alterations in BBB integrity using antibodies to occludin and ZO-1, fibrinogen, a serum protein that extravasates during BBB breakdown, and GFAP, an intermediate filament protein that increases in reactive astrocytes.

Blood vessels from control sections demonstrated strong, intravascular fibrinogen immunoreactivity in association with strong, continuous interendothelial reactivity for either tight junction protein. (ZO-1 immunostaining is shown in Figure 3A and throughout Figure 3. Similar reactivity patterns were seen with occludin immunostaining; data are not shown.) Although mild neuronal cross-reactivity for fibrinogen was observed in the globus pallidus (Figure 3C) and cerebellar dentate nucleus, significant perivascular fibrinogen extravasation was not observed in any region examined (Figure 2D). GFAP-reactive, parenchymal, and perivascular astrocytes and fibrillar cell processes were identified in the superficial cortex and cerebellum and, less frequently, in the deep gray matter and cortical white matter (Figure 3B). Alterations in tight junction proteins or their colocalization with GFAP-reactive cells or cell processes (Figure 3B) were not observed in any region. Furthermore, perivascular fibrinogen extravasation or its colocalization with GFAP-reactive cells or cell processes was not identified (Figure 3C).

Similarly, a majority of blood vessels from all HIV-1 sections showed strong, continuous interendothelial reactivity for the tight junction markers, occludin or ZO-1, in association with strong, intravascular immunoreactivity for fibrinogen. No statistically significant difference ($P > 0.05$) in vascular fibrinogen permeability was observed in any region compared to the same regions in control sections (Figure 2D). Scattered, isolated medium-sized

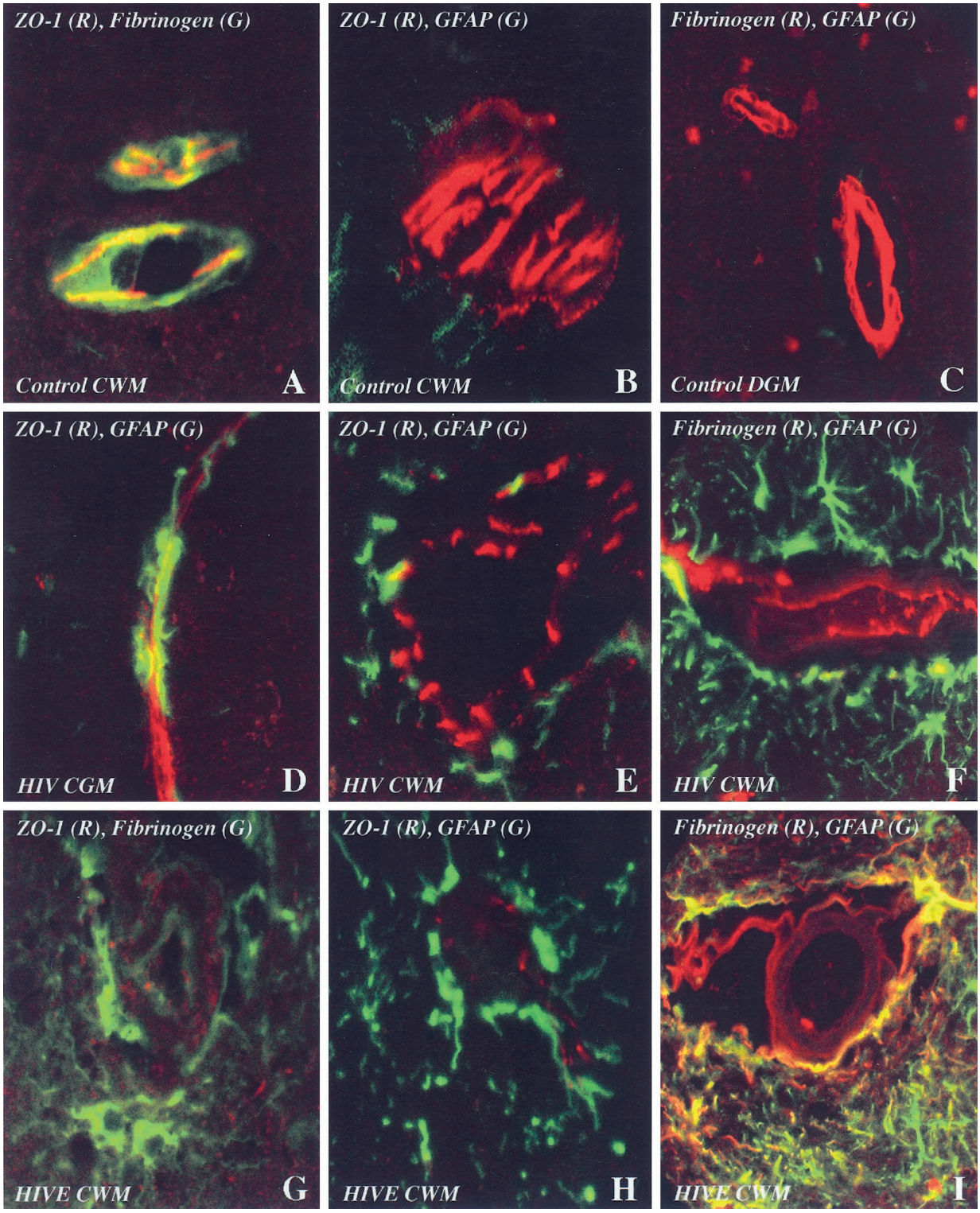

Figure 3. Tight junction protein disruption is associated with marked serum protein extravasation and astrocytosis in HIVE. **A–C:** In control sections, blood vessels display intact, ZO-1-positive tight junctions (red fluorochrome, **A** and **B**) and retain the intravascular serum protein, fibrinogen (green fluorochrome, **A**). Weakly staining, GFAP-reactive cell processes surround the intact BBB (green fluorochrome, **B** and **C**), however, do not overlap with either ZO-1-positive tight junctions (red fluorochrome, **B**) or intravascular fibrinogen (red fluorochrome, **C**). **D–F:** In HIV sections, scattered blood vessels with ZO-1-fragmented tight junctions (red fluorochrome, **D**) and, less often, intact ZO-1-positive tight junctions (red fluorochrome, **E**) overlap (yellow) with GFAP-reactive cell processes (green fluorochrome, **D** and **E**). In addition, GFAP-reactive astrocytes (green fluorochrome, **F**) colocalize focally (yellow) with extravasated fibrinogen (red fluorochrome, **F**) from the focally disrupted BBB. **G–I:** In HIVE sections, abundantly extravasated fibrinogen (green fluorochrome, **G**) and numerous hypertrophic, GFAP-reactive astrocytes (green fluorochrome, **H**), surround ZO-1-disrupted blood vessels (red fluorochrome, **G** and **H**). Colocalization of the two markers with ZO-1 is not observed due to extensive disruption of the tight junction protein (red fluorochrome, **G** and **H**). GFAP-reactive astrocytes (green fluorochrome, **I**), on the other hand, colocalize extensively (yellow) with extravasated fibrinogen (red fluorochrome, **I**) from the markedly disrupted BBB. Similar changes were observed in occludin immunostained sections. Double-label immunofluorescence laser confocal microscopy; original magnification, ×600. CGM, cortical gray matter; CWM, cortical white matter, DGM, deep gray matter.

blood vessels in the cortical white matter, the deep gray matter, and, less often, the cortical gray matter, however, showed tight junction protein fragmentation in association with perivascular astrocytosis (Figure 3D). GFAP-reactive, hypertrophic astrocytes surrounding the majority of these blood vessels colocalized focally with fragmented tight junction proteins (Figure 3D), as well as extravasated fibrinogen (Figure 3F). In addition, some GFAP-reactive, perivascular astrocytes in these regions colocalized focally with occludin- or ZO-1-positive vessels showing no apparent alterations in expression of these markers (Figure 3E).

In contrast, a majority of small and medium-sized blood vessels in the cortical white matter and deep gray matter from HIVE sections showed marked alterations in both the intensity and staining pattern of occludin and ZO-1 in association with abundant, perivascular fibrinogen extravasation, diffuse parenchymal fibrinogen immunoreactivity, and diffuse astrocytosis. Vessels with minimal to absent tight junction protein expression showed marked perivascular fibrinogen extravasation in these regions (Figure 3G). Similarly, vessels with disrupted tight junction proteins were accompanied by marked, diffuse perivascular and parenchymal astrocytosis (Figure 3H). GFAP-reactive hypertrophic astrocytes surrounding permeable blood vessels colocalized extensively with fibrinogen (Figure 3I), but not with occludin- or ZO-1-positive remnants (Figure 3H). The cortical gray matter showed similar, but less extensive, changes. All of these regions, however, demonstrated highly statistically significant decreases ($P \leq 0.0001$) in the mean number of blood vessels containing intravascular fibrinogen compared to the same regions in control or HIV-1 sections (Figure 2D).

Blood vessels in the cerebellar cortex and white matter from HIVE sections, on the other hand, showed only focal changes in tight junction protein integrity, accompanied by focal vascular fibrinogen permeability and perivascular astrocytosis. The extent of these alterations was similar to that seen in the cortical gray matter in HIV-1 sections. Likewise, no statistically significant difference ($P > 0.05$) was observed in the mean number of cerebellar blood vessels containing intravascular fibrinogen compared to the same regions in control or HIV-1 sections (Figure 2D).

Tight Junction Protein Disruption and BBB Permeability Are Associated with Mononuclear Cell Infiltrates and Microglial Nodules in HIVE

Sections were examined immunohistochemically for BBB alterations and their relationship to mononuclear cell and microglial aggregates using antibody to CD68, a marker for peripheral blood monocytes and tissue macrophages, including microglia. In addition, sections were analyzed for the expression of HLA-DR, a Class II major histocompatibility complex (MHC) activation marker, as well as gp41, an HIV-1 envelope protein expressed by a percentage of circulating viral-infected monocytes during HIV-1 infection.

All regions in control sections contained a small number of round CD68-reactive cells and short, CD68-reactive cell processes scattered throughout the parenchyma (data not shown). Infrequent blood vessels walls contained large CD68-positive infiltrating mononuclear cells that colocalized with tight junction proteins (ZO-1 immunostaining is shown in Figure 4A and throughout Figures 4 and 5; similar reactivity patterns were seen with occludin immunostaining, data not shown) and expressed Class II MHC molecules (Figure 5A). Less often, flattened periadventitial cells that did not colocalize with tight junction proteins were identified adjacent to the abluminal aspect of blood vessel walls. No alterations in tight junction protein expression (Figure 4A) or fibrinogen permeability (data not shown) were observed in any vessel wall. In addition, no viral protein expression was detected in any parenchymal or intravascular cell (data not shown).

Compared to control sections, HIV-1 sections demonstrated a mild increase in CD68-positive cells and cell processes (Figure 4B) within both the cortex and cerebellum. Furthermore, scattered gp41-positive cells were observed within the blood vessels walls and parenchyma of all sections examined (Figure 5D). Blood vessels that showed no alterations in tight junction protein expression or fibrinogen permeability were variably associated with CD68-positive (Figure 4B) or gp41-positive cells (Figure 5D). On the other hand, CD68-positive cells, both isolated and in small clusters, were consistently associated with scattered cerebral vessels showing tight junction protein fragmentation (Figure 4C) or fibrinogen permeability (Figure 4G). Despite expression by these cells of Class II MHC molecules, however, no overall increase in HLA-DR expression was observed in any region compared to the same region in control sections (Figure 5B).

Compared to both HIV-1 and control sections, HIVE sections demonstrated a marked increase in parenchymal and perivascular CD68-positive cells, including CD68-reactive microglial nodules, within the cortical white matter, the deep gray matter, and, to a lesser extent, the cortical gray matter (Figure 4D). Cerebellar sections, on the other hand, contained only a slightly greater number of immunoreactive cells than that observed in all HIV-1 sections (data not shown). In all regions, blood vessels with no alterations in tight junction protein expression or fibrinogen permeability were variably associated with CD68-positive cells (data not shown), similar to that observed in HIV-1 sections. In contrast, tight junction-disrupted and fibrinogen-permeable blood vessels were consistently associated with CD68-positive mononuclear cell aggregates or microglial nodules (Figure 4, D and H). Many of these disrupted blood vessels were surrounded, often asymmetrically, by clusters of hypertrophic, periadventitial CD68-reactive cells that variably colocalized with tight junction protein remnants (Figure 4E). More often, fragmented and permeable blood vessel walls were pavemented or infiltrated by colocalizing CD68-positive mononuclear cells, often in aggregates (Figure 4, F and I). A marked increase in Class II MHC expression was observed in these vascular- and perivascular-associated cells, as well as short ar-

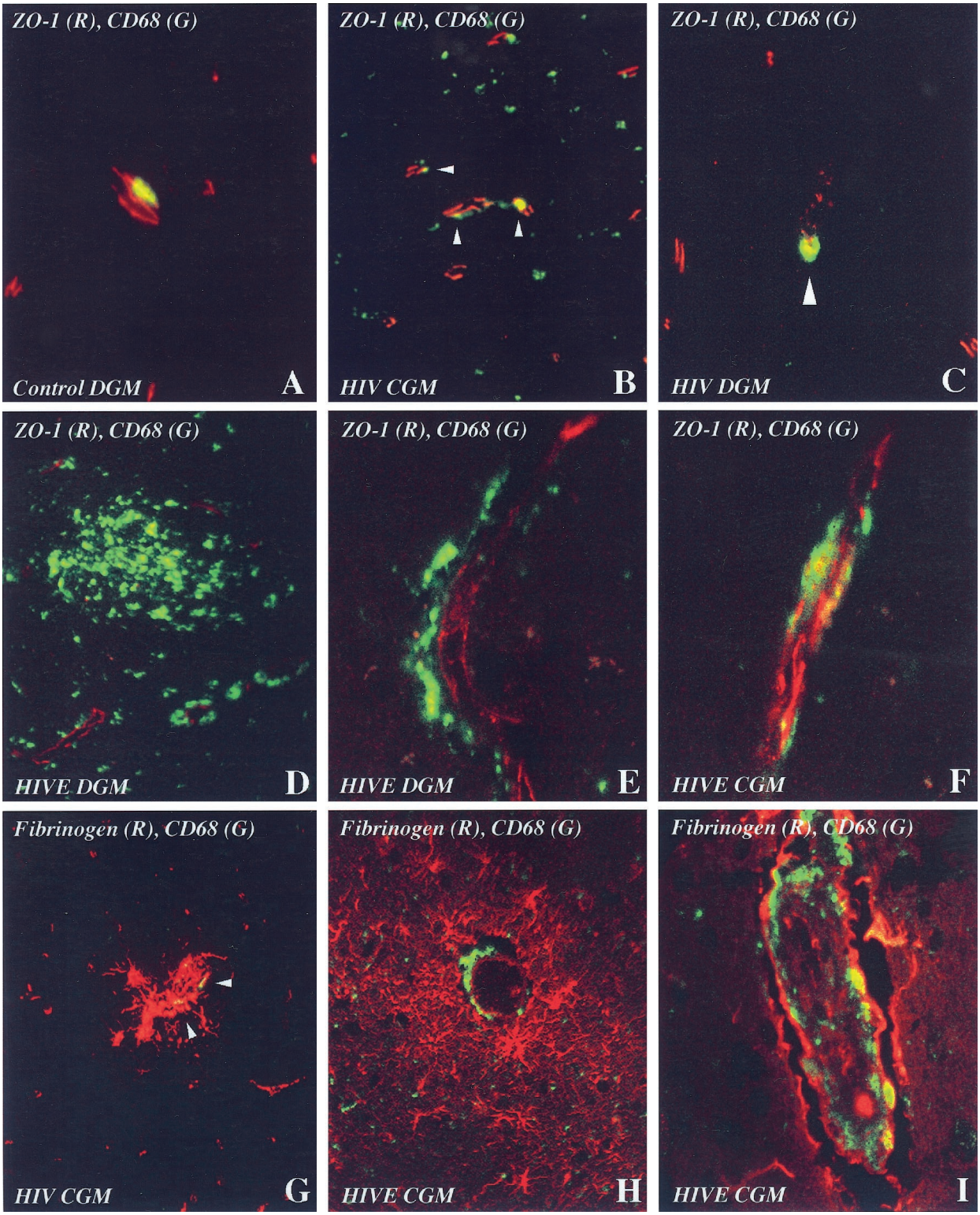

Figure 4. Tight junction protein disruption and BBB permeability are associated with mononuclear cell infiltrates and microglial nodules in HIVE. **A:** In control sections, infrequent blood vessels are infiltrated (yellow) by CD68-positive mononuclear cells (green fluorochrome) with no apparent disruption of ZO-1-positive tight junctions (red fluorochrome). **B, C,** and **G:** In HIV sections, increased CD68-positive mononuclear cells and microglial processes (green fluorochrome, **B**) are present among and colocalize focally (**arrowheads**, yellow) with ZO-1-positive blood vessels (red fluorochrome, **B**). In addition, scattered ZO-1-fragmented (red fluorochrome, **C**) and fibrinogen-permeable blood vessels (red fluorochrome, **G**) are infiltrated (**arrowheads**, yellow) by CD68-positive mononuclear cells (green fluorochrome, **C** and **G**). **D–F, H,** and **I:** In HIVE sections, numerous ZO-1-disrupted (red fluorochrome, **D**) and fibrinogen-permeable blood vessels (red fluorochrome, **H**) are associated with CD68-positive mononuclear cell aggregates and microglial nodules (green fluorochrome, **D** and **H**) and microglial nodules. CD68-reactive cells (green fluorochrome, **E, F,** and **I**) both surround (**E**) and infiltrate (yellow, **F** and **I**) the disrupted blood vessels (red fluorochrome: ZO-1, **E** and **F**; fibrinogen, **I**). Similar changes were observed in occludin-immunostained sections. **B, D, G,** and **H:** Double-label immunofluorescence laser confocal microscopy; original magnification, ×200. **A** and **C:** Double-label immunofluorescence laser confocal microscopy; original magnification, ×400. **E, F,** and **I:** Double-label immunofluorescence laser confocal microscopy, original magnification, ×600. CGM, cortical gray matter; DGM, deep gray matter.

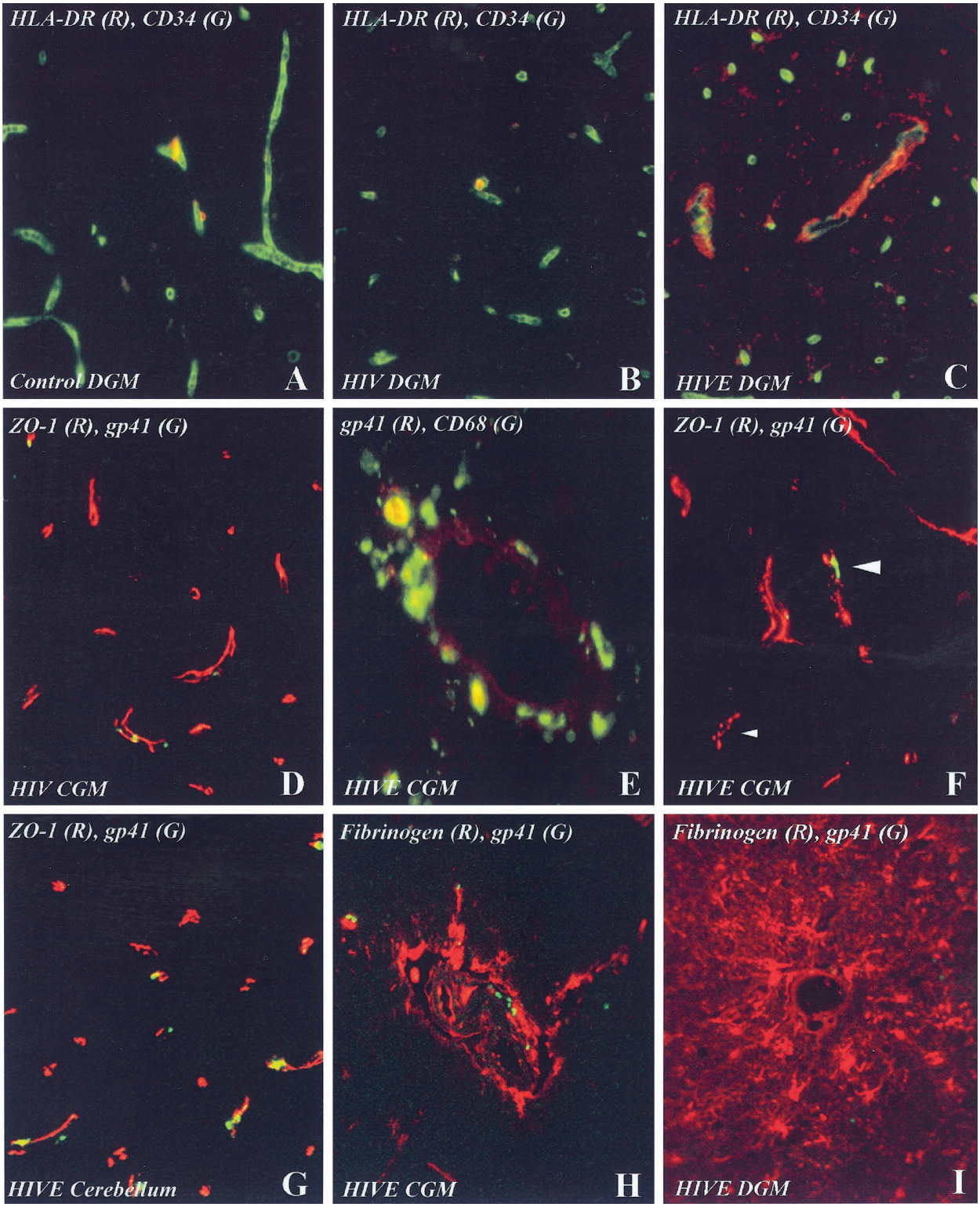

Figure 5. BBB disruption in HIVE is associated with mononuclear cell expression of Class II MHC activation markers but not HIV envelope protein. In control (**A**) and HIV (**B**) sections labeled for endothelial cells (green fluorochrome), infrequent infiltrating (yellow) mononuclear cells express the MHC Class II activation marker, HLA-DR (red fluorochrome). **C:** In HIVE sections, perivascular and parenchymal expression of the MHC Class II activation marker (red fluorochrome) is pronounced. **D:** In HIV sections, gp41-positive cells (green fluorochrome) infiltrate (yellow) and surround blood vessels with intact ZO-1-positive tight junctions (red fluorochrome). **E:** In HIVE sections, infiltrating CD68-positive mononuclear cells (green fluorochrome) colocalize focally (yellow) with the HIV envelope protein, gp41 (red fluorochrome). **F** and **G:** In HIVE sections, gp41-positive cells (green fluorochrome) associate with both intact and fragmented (**large arrowhead**) ZO-1-positive tight junctions (red fluorochrome). Likewise, some fragmented tight junctions show no association with gp41-positive cells (**small arrowhead, F**). **H–I:** In HIVE sections, fibrinogen-permeable blood vessels (red fluorochrome) are also variably associated with gp41-positive cells (green fluorochrome). **A–D, F,** and **G:** Double-label immunofluorescence microscopy; original magnification, ×200. **E:** Double-label immunofluorescence laser confocal microscopy, original magnification, ×600. **H** and **I:** Double-label immunofluorescence laser confocal microscopy, original magnification, ×200. CGM, cortical gray matter; DGM, deep gray matter.

borizing cell processes within the surrounding parenchyma (Figure 5C).

In contrast to the regional differences in CD68 reactivity, a similar difference was not observed in the number of gp41-positive cells within the cortex and cerebellum of HIVE sections (Figure 5, F and G). Although both areas contained a greater number of gp41-positive cells compared to HIV-1 sections, significant tight junction protein alterations were not observed in vessels within the cerebellum, despite focal vascular infiltration by gp41-positive cells (Figure 5G). Furthermore, viral proteins were not consistently observed among fragmented (Figure 5F) or permeable vessels of the cerebrum (Figure 5, H and I), despite focal colocalization with CD68-reactive mononuclear cells within blood vessel walls (Figure 5E).

Discussion

HIV-1-associated dementia complex is characterized histologically by an invasion of large numbers of infected monocytes into the CNS late in the course of the disease.[13] Previous studies have demonstrated that the BBB, which normally regulates cell trafficking into the CNS parenchyma, is compromised in HIVE[36,41,42] and that this alteration may occur as a result of interactions with activated monocytes and their soluble products.[51,52] The actual basis of the disruption, however, has not been elucidated. We now report that highly significant disruptions in BBB tight junctions, as demonstrated by immunohistochemical changes in the expression and distribution of the proteins, occludin and ZO-1, occur during HIVE. We further demonstrate that these alterations occur in CNS regions susceptible to histopathological damage in association with serum protein extravasation, astrocytosis, and the accumulation of activated, HIV-1-infected monocytes and microglia. Together, these data suggest that intercellular conduits created by the disruption of BBB tight junctions may serve as the pathological mechanism whereby HIV-1-infected monocytes gain significant access to the CNS.

Our results clearly demonstrate that tight junction alterations correlate with serum protein extravasation, underscoring the importance of this critical structure in maintaining the relative impermeability of the BBB. The demonstration of widespread serum protein extravasation in HIVE is in agreement with previous reports[36] but in contrast to others, which did not detect a difference in BBB permeability between brain tissue from HIV-1-infected patients with and without encephalitis.[42] This disparity may be a reflection of the more sensitive immunohistochemical techniques employed in this study. The focal tight junction disruption and serum protein extravasation observed in the frontal cortex and basal ganglia from HIV-infected patients contrasts sharply with the extensive changes seen in these regions from HIV-infected patients with encephalitis. These findings support the idea that BBB permeability changes develop slowly and precede the onset of HIVE,[36] which occurs late in the course of infection. These findings also suggest that permeability changes may contribute directly to the CNS injury observed in HIVE. Distention of the extracellular space by vasogenic edema may contribute to alterations in the ionic milieu and, in turn, cellular membrane function.[36]

In addition, the development of astrocytosis, a prominent feature that accompanied tight junction and permeability alterations in this study, may play a dual role in both protecting the CNS from BBB-induced alterations and augmenting loss of BBB integrity. Astrocytosis is consistently reported as the earliest neuropathologic change in the CNS of HIV-1-infected patients.[53] The relationship between focal BBB compromise and perivascular astrocytosis in HIV-1 tissue in this report suggests that this reactive change is triggered by loss of BBB integrity and serves, initially, to wall off impending damage to the CNS microenvironment. Reactive astrocytes, however, are potent mediators of vascular permeability-inducing cytokines, including tumor necrosis factor-α (TNF-α) and interleukin-6 (IL-6), which may augment permeability changes with time.[54,55] Furthermore, under physiological conditions, astrocytes play a critical role in maintaining tight junction integrity,[56] a role that may be compromised during gliosis. These possibilities are intriguing in light of the observation that focal overlap of GFAP-reactive processes and tight junction proteins was observed in vessels without light microscopic evidence of BBB perturbations in tissue from HIV-1-infected patients without encephalitis.

On the other hand, the presence of comparable numbers of gp41-infected monocytes within both affected and unaffected cerebral and cerebellar vessels in HIVE strongly suggests that the presence of this HIV-1 envelope protein, by itself, is not sufficient for tight junction modulation or permeability alterations during this disease. Other HIV-1 proteins, however, may play a role in compromising tight junction integrity, as supported by the demonstration that the HIV-1 envelope protein, gp120, can induce intercellular gaps in rat brain endothelium through a mechanism that may involve substance P.[57] Although the direct transmission of HIV-1 through endothelial cells of the BBB remains controversial,[51,58–61] reports of gp120 adsorptive endocytosis across cerebral endothelial cells *in vitro*[62,63] suggest that this pathway may also constitute a significant route of viral entry into the CNS.

Our findings, on the other hand, lend credence to the hypothesis that HIV-1-infected monocytes play an essential role in breaching the BBB,[51,52,64] thus, facilitating both neurotoxicity[14–18] and viral transmission into the CNS.[51,65] Several lines of evidence indicate that the local production of monocyte-generated cytokines, in particular TNF-α, are the most likely candidates for mediating tight junction disruption after the adherence of activated monocytes to the cerebral vascular lining. TNF-α and interferon-γ induce a striking fragmentation of ZO-1 via F actin rearrangement in cultures of microvascular endothelial cells.[66] Indeed, high levels of these cytokines are present in the CNS of patients with HIV-1-associated dementia complex.[67] In addition, activated monocytes adhere and migrate readily through interendothelial gaps in artificial BBB systems, in association with their produc-

tion of high levels of pro-inflammatory cytokines, including TNF-α.[52,68]

In addition, the cerebral endothelial lining itself may play an important role in determining sites of inflammation through its phenotypic and antigenic diversity. This is supported by our finding that tight junction alterations were confined to small and medium-sized vessels within the subcortical white matter and basal ganglia in HIVE. An accumulating body of evidence strongly indicates that the selective expression of adhesion molecules by different caliber vessels within different regions of the CNS may contribute to site-specific inflammation observed in various encephalitides. In studies of HIV-1-infected monocytes, up-regulation of endothelial E-selectin and VCAM-1 by these activated cells and their soluble products promotes their avid adherence to cerebral endothelial cells *in vitro.*[51] Furthermore, capillary up-regulation of these molecules occurs in HIVE in association with infiltrating mononuclear cells, in contrast to ubiquitous up-regulation of ICAM-1 by both endothelial and parenchymal cells.[51]

In summary, the results of this study demonstrate that significant, site-specific alterations in tight junction integrity occur during HIVE and are associated with marked BBB permeability, activated HIV-1-infected monocyte accumulation, and astrocytosis. Further investigation of the precise molecules and mechanisms that disrupt this critical barrier structure may be of value in abrogating CNS injury, as well as the paracellular migration of activated HIV-1 monocytes in the CNS, critical events in the pathogenesis of HIV-1-associated dementia.

References

1. Janssen RS, Cornblath DR, Epstein LG, Foa RP, McArthur JC, Price RW, Asbury AKK, Beckett A, Benson DF, Bridge TP, Leventhal CM, Satz P, Saykin AJ, Sidtiss JJ, Tross S: Nomenclature and research case definitions for neurological manifestations of human immunodeficiency virus type-1 (HIV-1) infection. Neurology 1991, 41:778–785
2. Navia BA, Jordan BD, Price RW: The AIDS dementia complex. I. Clinical features. Ann Neurol 1986, 19:517–524
3. Price RW, Brew B, Sidtis J, Rosenblum M, Schneck AC, Cleary P: The brain and AIDS: central nervous system HIV-1 infection and AIDS dementia complex. Science 1988, 239:586–592
4. AAN Task Force: Nomenclature and research case definitions for neurologic manifestations of human immunodeficiency virus-type 1 (HIV-1) infection. Report of a Working Group of the American Academy of Neurology AIDS Task Force. Neurology 1991, 41:778–785
5. Navia BA, Cho ES, Petito CK, Price PW: The AIDS dementia complex. II. Neuropathology. Ann Neurol 1986, 19:525–535
6. Wiley CA, Masliah E, Morey M, Lemere C, DeTeresa R, Grafe M, Hansen L, Terry R: Neocortical damage during HIV infection. Ann Neurol 1991, 29:651–657
7. Budka H: Neuropathology of human immunodeficiency virus infection. Brain Pathol 1991, 1:163–175
8. Wiley CA, Achim CL: Human immunodeficiency virus encephalitis is the pathological correlate of dementia in acquired immunodeficiency syndrome. Ann Neurol 1994, 36:673–676
9. Epstein LG, Sharer LR, Cho ES, Myenhofer M, Navia BA, Price RW: HTLV-III/LAV-like retrovirus particles in the brains of patients with AIDS encephalopathy. AIDS Res 1984, 1:447–454
10. Koenig S, Gendelman HE, Orenstein JM, Dal Canto MC, Pezeshkpour GH, Yungbluth M, Janotta F, Aksamit A, Martin MA, Fauci AS: Detection of AIDS virus in macrophages in brain tissue from AIDS patients with encephalopathy. Science 1986, 233:1089–1093
11. Wiley CA, Schrier RD, Nelson JA, Lampert PW, Oldstone MBA: Cellular localization of human immunodeficiency virus infection within the brains of acquired immune deficiency syndrome patients. Proc Natl Acad Sci USA 1986, 83:7089–7093
12. Stoler MH, Eskin TA, Benn S, Angerer RC, Angerer LM: Human T-cell lymphotropic virus type III infection of the central nervous system: a preliminary in situ analysis. JAMA 1986, 256:2360–2364
13. Glass JD, Fedor H, Wesselingh SL, McArthur JC: Immunocytochemical quantitation of human immunodeficiency virus in the brain: correlations with dementia. Ann Neurol 1995, 38:755–762
14. Giulian D, Vaca K, Noonan CA: Secretion of neurotoxins by mononuclear phagocytes infected with HIV-1. Science 1990, 250:1593–1596
15. Pulliam L, Herndier BG, Tang NM, McGrath MS: Human immunodeficiency virus-infected macrophages produce soluble factors that cause histological and neurochemical alterations in cultured human brains. J Clin Invest 1991, 87:503–512
16. Tardieu M, Hery C, Peudenier S, Boespflug O, Montagnier L: Human immunodeficiency virus type 1-infected monocytic cells can destroy human neural cells after cell-to-cell adhesion. Ann Neurol 1992, 32: 11–17
17. Genis P, Jett M, Bernton EW, Boyle T, Gelbard HA, Dzenko K, Keane RW, Resnick L, Mizrachi Y, Volsky DJ, Epstein LG, Gendelman HE: Cytokines and arachidonic metabolites produced during human immunodeficiency virus (HIV)-infected macrophage-astroglia interactions: implications for the neuropathogenesis of HIV disease. J Exp Med 1992, 176:1703–1718
18. Giulian D, Wendt E, Vaca K, Noonan CA: The envelope glycoprotein of human immunodeficiency virus type 1 stimulates release of neurotoxins from monocytes. Proc Natl Acad Sci USA 1993, 90:2769–2773
19. Nottet HSLM, Gendelman HE: Unraveling the neuroimmune mechanisms for the HIV-1 associated cognitive/motor complex. Immunol Today 1995, 16:441–448
20. Hirano A: The organization of the astrocyte-microvascular interface. Stroke and Microcirculation. Edited by Cervos-Navarro J, Ferst R. New York, Raven Press, 1987, pp 219–222
21. Pardridge WM: Recent advances in blood-brain barrier transport. Annu Rev Pharmacol Toxicol 1988, 28:25–39
22. Coomber BL, Stewart PA: Morphometric analysis of CNS microvascular endothelium. Microvasc Res 1985, 30:99–115
23. Reese TS, Karnovsky MJ: Fine structural localization of a blood-brain barrier for exogenous peroxidase. J Cell Biol 1967, 34:207–217
24. Brightman MW, Reese TJ: Junctions between intimately apposed cell membranes in the vertebrate brain. J Cell Biol 1969, 40:648–677
25. Staehelin LA: Structure and function of intercellular junctions. Int Rev Cytol 1974, 39:191–283
26. Furuse M, Hirase T, Itoh M, Nagafuchi A, Yonemura S, Tsukita S, Tsukita S: Occludin: a novel integral membrane protein localizing at tight junctions. J Cell Biol 1993, 123:1777–1788
27. Hirase T, Staddon JM, Saitou M, Ando-Akatsuka Y, Itoh M, Furuse M, Fujimoto K, Tsukita S, Rubin LL: Occludin as a possible determinant of tight junction permeability in endothelial cells. J Cell Sci 1997, 110:1603–1613
28. Watson PM, Anderson JM, Vanltallie CM, Doctrow SR: The tight-junction-specific protein ZO-1 is a component of the human and rat blood-brain barriers. Neurosci Lett 1991, 129:6–10
29. Farrell CL, Shivers RR: Capillary junctions of the rat are not affected by osmotic opening of the blood-brain barrier. Acta Neuropathol (Berl) 1984, 63:179–189
30. Schielke E, Tatsch K, Pfister HW, Trenkwalder C, Leinsinger G, Kirsch CM, Matuschke A, Einhaupl KM: Reduced cerebral blood flow in early stages of human immunodeficiency virus infection. Arch Neurol 1990, 47:1342–1345
31. Tran Dinh YR, Mamo H, Cervoni J, Caulin C, Saimot AC: Disturbances in the cerebral perfusion of human immune deficiency virus-1 seropositive asymptomatic subjects: a quantitative tomography study of 18 cases. J Nucl Med 1990, 31:1601–1607
32. Masdeu JC, Yudd A, Van Heertum RL, Grundman M, Hriso E, O'Connell RA, Luck D, Camli U, King LN: Single-photon emission computed tomography in human immunodeficiency virus encephalopathy: a preliminary report. J Nucl Med 1991, 32:1471–1475
33. Olsen WL, Longo FM, Mills CM, Norman D: White matter disease in AIDS: findings at MR imaging. Radiology 1988, 169:445–448

34. Balakrishnan J, Becker PS, Kumar AJ, Zinreich SJ, McArthur JC, Bryan RN: Acquired immunodeficiency syndrome: correlation of radiologic and pathologic findings in the brain. Radiographics 1990, 10:201–215
35. Flowers CH, Mafee MF, Crowell R, Raofi B, Arnold P, Dobben G, Wycliffe N: Encephalopathy in AIDS patients: evaluation with MR imaging. Am J Neuroradiol 1990, 11:1235–1245
36. Power C, Kong PA, Crawford TO, Wesselingh S, Glass JD, McArthur JC, Trapp BD: Cerebral white matter changes in acquired immunodeficiency syndrome dementia: alterations of the blood-brain barrier. Ann Neurol 1993, 34:339–350
37. Marshall DW, Brey RL, Butzin CA, Lucey DR, Abbadessa SM, Boswell RN: CSF changes in a longitudinal study of 124 neurologically normal HIV-1-infected U.S. Air Force personnel. J Acquir Immune Defic Syndr 1991, 4:777–781
38. McArthur JC, Nance-Sproson TE, Griffin DE, Hoover D, Selnes OA, Miller EN, Margolick JB, Cohen BA, Farzadegan H, Saah A: The diagnostic utility of elevation in cerebrospinal fluid beta 2-microglobulin in HIV-1 dementia. Multicenter AIDS Cohort Study. Neurology 1992, 42:1707–1712
39. Sporer B, Paul R, Koedel U, Grimm R, Wick M, Goebel FD, Pfister HW: Presence of matrix metalloproteinase-9 activity in the cerebrospinal fluid of human immunodeficiency virus-infected patients. J Infect Dis 1998, 178:854–857
40. Giovannoni G, Miller RF, Heales SJ, Land JM, Harrison MJ, Thompson EJ: Elevated cerebrospinal fluid and serum nitrate and nitrite levels in patients with central nervous system complications of HIV-1 infection: a correlation with blood-brain-barrier dysfunction. J Neurol Sci 1998, 156:53–58
41. Rhodes RH: Evidence of serum-protein leakage across the blood-brain barrier in the acquired immunodeficiency syndrome. J Neuropathol Exp Neurol 1991, 50:171–183
42. Petito CK, Cash KS: Blood-brain barrier abnormalities in the acquired immunodeficiency syndrome: immunohistochemical localization of serum proteins in postmortem brain. Ann Neurol 1992, 32:658–666
43. Smith TW, DeGirolami U, Henin D, Bolgert F, Hauw JJ: Human immunodeficiency virus (HIV) leukoencephalopathy and the microcirculation. J Neuropathol Exp Neurol 1990, 49:357–370
44. Büttner A, Mehraein P, Weis S: Vascular changes in the cerebral cortex in HIV-1 infection: II. An immunohistochemical and lectin histochemical investigation. Acta Neuropathol 1996, 92:35–41
45. Weis S, Haug H, Budka H: Vascular changes in the cerebral cortex in HIV-1 infection: I. A morphometric investigation by light and electron microscopy. Clin Neuropathol 1996, 15:361–366
46. Kovitz CA, Morgello S: Cerebral glucose transporter expression in HIV infection. Acta Neuropathol 1997, 94:140–145
47. Wiley CA, Soontornniyomkij V, Radhakrishnan L, Masliah E, Mellors J, Hermann SA, Dailey P, Achim CA: Distribution of brain HIV load in AIDS. Brain Pathol 1998, 8:277–284
48. Soontornniyomkj V, Nieto-Rodríguez JA, Martínez AJ, Kingsley LA, Achim CL, Wiley CA: Brain HIV burden and length of survival after AIDS diagnosis. Clin Neuropathol 1998, 17:95–99
49. Stevenson BR, Siliciano JD, Mooseker MS, Goodenough DA: Identification of ZO-1: a high molecular weight polypeptide associated with the tight junction (zonula occludens) in a variety of epithelia. J Cell Biol 1986, 103:755–766
50. Howarth AG, Stevenson BR: Molecular environment of ZO-1 in epithelial and non-epithelial cells. Cell Motil Cytoskeleton 1995, 31: 323–332
51. Nottet HSLM, Persidsky Y, Sasseville VG, Nukuna AN, Bock P, Zhai QH, Sharer LR, McComb RD, Swindells S, Soderland C, Gendelman HE: Mechanisms for the transendothelial migration of HIV-1-infected monocytes into brain. J Immunol 1996, 156:1284–1295
52. Persidsky Y, Stins M, Way D, Witte MH, Weinand M, Kim KS, Bock P, Gendelman HE, Fiala M: A model for monocyte migration through the blood-brain barrier during HIV-1 encephalitis. J Immunol 1997, 158: 3499–3510
53. Vitkovic L, da Cunha A: Role for astrocytosis in HIV-1-associated dementia. Curr Top Microbiol Immunol 1995, 202:105–116
54. Brett FM, Mizisin AP, Powell HC, Campbell IL: Evolution of neuropathologic abnormalities associated with blood-brain barrier breakdown in transgenic mice expressing interleukin-6 in astrocytes. J Neuropathol Exp Neurol 1995, 54:766–775
55. Ridet JL, Malhotra SK, Privat A, Gage FH: Reactive astrocytes: cellular and molecular cues to biological function. Trends Neurosci 1997, 20:570–577
56. Janzer RC, Raff MC: Astrocytes induce blood-brain barrier properties in endothelial cells. Nature 1987, 325:253–257
57. Annunziata P, Cioni C, Toneatto S, Paccagnini E: HIV-1 gp120 increases the permeability of rat brain endothelium cultures by a mechanism involving substance P. AIDS 1998, 12:2377–2385
58. Moses AV, Bloom FE, Pauza CD, Nelson JA: Human immunodeficiency virus infection of human brain capillary endothelial cells occurs via a CD4/galactosylceramide-independent mechanism. Proc Natl Acad Sci USA 1993, 90:10474–10478
59. Power C, McArthur JC, Johnson RT, Griffin DE, Glass JD, Perryman S, Chesebro B: Demented and nondemented patients with AIDS differ in brain-derived human immunodeficiency virus type 1 envelope sequences. J Virol 1994, 68:4643–4649
60. Korber BT, Kunstman KJ, Patterson BK, Furtado M, McEvilly MM, Levy R, Wolinsky SM: Genetic differences between blood- and brain-derived viral sequences from human immunodeficiency virus type 1-infected patients: evidence of conserved elements in the V3 region of the envelope protein of brain-derived sequences. J Virol 1994, 68:7467–7481
61. Poland SD, Rice GPA, Dekaban GA: HIV-1 infection of human brain-derived microvascular endothelial cells in vitro. J Acquir Immune Defic Syndr Hum Retro 1995, 8:437–445
62. Banks WA, Kastin AJ, Akerstrom V: HIV-1 protein gp120 crosses the blood-brain barrier: role of adsorptive endocytosis. Life Sci 1997, 61:PL119–125
63. Banks WA, Akerstrom V, Kastin AJ: Adsorptive endocytosis mediates the passage of HIV-1 across the blood-brain barrier: evidence for a post-internalization coreceptor. J Cell Sci 1998, 111:533–540
64. Nottet HS, Bar DR, van Hassel H, Verhoef J, Boven LA: Cellular aspects of HIV-1 Infection of macrophages leading to neuronal dysfunction in in vitro models for HIV-1 encephalitis. J Leukoc Biol 1997, 62:107–116
65. Peluso R, Haase A, Stowring L, Edwards M, Ventura P: A Trojan horse mechanism for the spread of visna virus in monocytes. Virology 1985, 147:231–236
66. Blum MS, Toninelli E, Anderson JM, Balda MS, Zhou J, O'Donnell L, Pardi R, Bender JR: Cytoskeletal rearrangement mediates human microvascular endothelial tight junction modulation by cytokines. Am J Physiol 1997, 273:H286–294
67. Griffin DE: Cytokines in the brain during viral infection: clues to HIV-associated dementia. J Clin Invest 1997, 100:2948–2951
68. Fiala M, Looney DJ, Stins M, Way DD, Zhang L, Gan X, Chiappelli F, Schweitzer ES, Shapshak P, Weinand M, Graves MC, Witte M, Kim KS: TNF-alpha opens a paracellular route for HIV-1 invasion across the blood-brain barrier. Mol Med 1997, 3:553–564